



This is a repository copy of *Temperature dependent dielectric and Raman spectra and microwave dielectric properties of gehlenite-typed Ca<sub>2</sub>Al<sub>2</sub>SiO<sub>7</sub> ceramics*.

White Rose Research Online URL for this paper:  
<https://eprints.whiterose.ac.uk/153045/>

Version: Accepted Version

---

**Article:**

Song, Z., Song, K., Liu, B. et al. (7 more authors) (2020) Temperature dependent dielectric and Raman spectra and microwave dielectric properties of gehlenite-typed Ca<sub>2</sub>Al<sub>2</sub>SiO<sub>7</sub> ceramics. *International Journal of Applied Ceramic Technology*, 17 (2). pp. 771-777. ISSN 1546-542X

<https://doi.org/10.1111/ijac.13414>

---

This is the peer reviewed version of the following article: Song, Z. , Song, K. , Liu, B. , Zheng, P. , Bafrooei, H. B., Su, W. , Lin, H. , Shi, F. , Wang, D. and Reaney, I. (2019), Temperature dependent dielectric and Raman spectra and microwave dielectric properties of gehlenite-typed Ca<sub>2</sub>Al<sub>2</sub>SiO<sub>7</sub> ceramics. *Int J Appl Ceram Technol.*, which has been published in final form at <https://doi.org/10.1111/ijac.13414>. This article may be used for non-commercial purposes in accordance with Wiley Terms and Conditions for Use of Self-Archived Versions.

**Reuse**

Items deposited in White Rose Research Online are protected by copyright, with all rights reserved unless indicated otherwise. They may be downloaded and/or printed for private study, or other acts as permitted by national copyright laws. The publisher or other rights holders may allow further reproduction and re-use of the full text version. This is indicated by the licence information on the White Rose Research Online record for the item.

**Takedown**

If you consider content in White Rose Research Online to be in breach of UK law, please notify us by emailing [eprints@whiterose.ac.uk](mailto:eprints@whiterose.ac.uk) including the URL of the record and the reason for the withdrawal request.



[eprints@whiterose.ac.uk](mailto:eprints@whiterose.ac.uk)  
<https://eprints.whiterose.ac.uk/>

# Temperature dependent dielectric and Raman spectra and microwave dielectric properties of gehlenite-typed $\text{Ca}_2\text{Al}_2\text{SiO}_7$ ceramics

Zhengjun Song<sup>1</sup>, Kaixin Song<sup>1,5,\*</sup>, Bing Liu<sup>1</sup>, Peng Zheng<sup>1</sup>, Hadi Barzegar Bafrooei<sup>1</sup>, Weitao Su<sup>2</sup>, Huixing Lin<sup>3,\*</sup>, Feng Shi<sup>4</sup>, Dawei Wang<sup>5,\*</sup>, I.M.Reaney<sup>5</sup>

<sup>1</sup> College of electronics information, Hangzhou Dianzi University, Hangzhou 310018, China.

<sup>2</sup> College of materials sciences and environmental engineering, Hangzhou Dianzi University, Hangzhou 310018, China.

<sup>3</sup> Shanghai institutes of ceramics, Chinese academy of sciences, 1295 Dingxi Road, Shanghai 200050, China.

<sup>4</sup> Department of materials sciences and engineering, Shandong University of sciences and technology, Qingdao 266590, China.

<sup>5</sup> Department of materials sciences and engineering, The University of Sheffield, Sheffield S1 3JD, U.K.

## ABSTRACT

Gehlenite-typed  $\text{Ca}_2\text{Al}_2\text{SiO}_7$  ceramics were prepared by the conventional solid-state reaction. Two anomalies were found in the plot of dielectric constant vs. temperature, which was associated to space charge polarization. Pure phase crystal structure and no phase transition were observed in the temperature dependent XRD patterns and Raman spectra from room temperature to 900°C. **There were relevant relation between  $Q \times f$  and  $\tau_f$  with the stretching vibrations of Ca-O bond and O-Ca-O bending in  $\text{CaO}_8$  polyhedron. Excellent microwave dielectric properties ( $\epsilon_r = 8.86$ ,  $Q \times f = 22,457\text{GHz}$ , and  $\tau_f = -51.06 \text{ ppm}/^\circ\text{C}$ ) were obtained for  $\text{Ca}_2\text{Al}_2\text{SiO}_7$  sintered at 1440°C in air, which had the potential application to use in microwave and millimeter-wave devices such as capacitors and substrates.**

**Keywords:** Silicate dielectrics, 5G, Microwave ceramics

---

\*Corresponding Authors: Email: kxsong@hdu.edu.cn; huixinglin@mail.sic.ac.cn; dawei.wang@sheffield.ac.uk

## 1 Introduction

Microwave dielectric ceramics are mainly used in various wireless communication systems such as resonators, filters, antennae, microstrip line and substrates [1, 2]. With the rapid development of wireless communication from 2G/3G/4G to 5G and beyond (higher frequency band with millimeter wave) techniques, microwave dielectric ceramics are desired to meet more requirements, which pushes the explore and development of new materials. Microwave dielectric ceramics with both low permittivity ( $\epsilon_r$ ) and low loss ( $\tan\delta$ ) are of great concern due to their low time delay of signal transmission, which are generally used in many 5G high-frequency applications (6-100 GHz) including satellite communications, Internet of things, and self-drive vehicles. Meanwhile, some non-linear dielectric materials are required with the high Curie temperature ( $T_c$ ) and a low dielectric loss ( $\tan\delta$ ) in 5G microwave and millimeter-wave devices such as capacitors and substrates [3].

Many new ceramic materials have been reported as microwave substrates, such as olivine type  $\text{Ca}_2\text{GeO}_4$  [4],  $\text{LiAl}_{1-x}(\text{Zn}_{0.5}\text{Si}_{0.5})_x\text{O}_2$  [5],  $\text{Eu}_2\text{Zr}_3(\text{MoO}_4)_9$  [6], etc. In them, silicate ceramics have received much attention due to their low permittivity materials with high quality factor ( $Q \times f$ ) values, such as  $\text{Zn}_{1.95}\text{M}_{0.05}\text{SiO}_4$  ( $M = \text{Zn}, \text{Mg}, \text{Ni}, \text{and Co}$ ) [7],  $\text{Zn}_2\text{GeO}_4$  [8], forsterite ( $\text{Mg}_{1-x}\text{Ni}_x$ ) $_2\text{SiO}_4$  [9]. Due to strong covalent bond in the basic unit of the  $[\text{SiO}_4]$  tetrahedral, the silicate ceramic material usually has a low dielectric constant, which has the potential to be used as microwave substrate [10]. Zou et al., reported there were weak ferroelectricity and excellent microwave dielectric properties of  $\text{Ba}_2\text{ZnSi}_2\text{O}_7$  ceramic with  $\epsilon_r = 8.09$ ,  $Q \times f = 26,634 \text{ GHz}$ , and  $\tau_f = -51.46\text{ppm}/^\circ\text{C}$  [11]. Gehlenite  $\text{Ca}_2\text{Al}_2\text{SiO}_7$  was an anamorphous of  $\text{AB}_2\text{Si}_2\text{O}_7$  by Al substitution of Si [12]. H. Takeda et al., studied on  $\text{Ca}_2\text{Al}_2\text{SiO}_7$  single crystal was applicable to piezoelectric sensors at high temperature [13]. N. Pelletier-Allard et al. reported site selective spectroscopy of Nd ions in gehlenite ( $\text{Ca}_2\text{Al}_2\text{SiO}_7$ ) for a new laser material [14]. Meanwhile, few people study the

microwave dielectric properties and temperature dependent dielectric spectra and structural evolution by adjusting the design of  $[\text{Si}_2\text{O}_7]$  silicate structural units in  $\text{AB}_2\text{Si}_2\text{O}_7$  ceramics.

Considering above situation, in this work, Al was used to replace Si in  $\text{AB}_2\text{Si}_2\text{O}_7$  to form  $\text{Ca}_2\text{Al}_2\text{SiO}_7$ , isomorphous to  $\text{Ba}_2\text{ZnSi}_2\text{O}_7$  crystal structure. The dependence of crystal structure, dielectric behaviors of  $\text{Ca}_2\text{Al}_2\text{SiO}_7$  ceramics on temperature, and microwave properties have been investigated in detail, by the employment of temperature *in-situ* XRD, Raman spectra, dielectric spectra ( $\epsilon_r$ -T).

## 2 Experimental procedure

$\text{Ca}_2\text{Al}_2\text{SiO}_7$  ceramics were synthesized by a traditional solid-state reaction method using high-purity chemicals of  $\text{CaCO}_3$  (99.0%),  $\text{Al}_2\text{O}_3$  (99.99%), and  $\text{SiO}_2$  (99.99%). According to the chemical formula, raw materials were weighed and ball-milled 24h using  $\text{ZrO}_2$  as media and deionized water as solvent. After dried at  $90^\circ\text{C}$ , the mixtures were calcined in air at  $1200^\circ\text{C}$  for 4 h with a heating rate of  $4^\circ\text{C}/\text{min}$ . And then the calcined powders were re-milled for 24h. The dried powders were uniaxially pressed into pellet samples with 15 mm in diameter, and 1 mm (for the measurement of  $\epsilon_r$ -T curves and Raman spectra) and 7 mm (for the measurement of microwave dielectric properties) in height under a pressure of 100 MPa. Then, the samples were sintered at  $1380^\circ\text{C}$  -  $1460^\circ\text{C}$  for 4h at a heating rate of  $4^\circ\text{C}/\text{min}$  in air.

The bulk densities of sintered samples were measured by the Archimedes method. The microstructure was revealed by a scanning electron microscope (SEM, JEOL JSM6380-LV, Tokyo, Japan). The grain size was calculated according to the SEM images using the software of Image J. The crystal structure was obtained via the X-ray diffraction (XRD, XRD-7000, Shimadzu, Kyoto, Japan) using  $\text{CuK}_\alpha$  radiation. **The *in-situ* temperature-dependent XRD patterns were acquired by a Siemens D5000 HTXRD in the temperature range  $30^\circ\text{C}$ - $900^\circ\text{C}$ .** The Raman was acquired by a Renishaw inVia Raman microscope in the temperature

range 100°C-600°C. Full-spectrum fitting of Rietveld refinement was performed by the GSAS and EXPGUI software [15, 16]. The temperature-dependent dielectric permittivity from room temperature (RT) to 1000°C was measured using an Agilent 4294A impedance analyzer (Agilent, Santa Clara, USA). The microwave dielectric properties were measured using the TE01 $\delta$  dielectric resonator method with a vector network analyzer (E8362B, Agilent Technologies, Palo Alto, CA). The temperature coefficient of resonance frequency ( $\tau_f$ ) was evaluated in the temperature range of 25°C-85°C was calculated by following formula:

$$\tau_f = \frac{f(T_1) - f(T_0)}{f(T_0) \times (T_1 - T_0)} \times 10^6 \text{ ppm/}^\circ\text{C} \quad (1)$$

Where  $f(T_1)$  and  $f(T_0)$  are the resonant frequencies at the measuring temperatures of  $T_1$  (85°C) and  $T_0$  (25°C), respectively.

### 3 Results and discussion

The full-spectrum fitting of Rietveld refinement for  $\text{Ca}_2\text{Al}_2\text{SiO}_7$  is shown in **Fig. 1**, with low values of refined parameters:  $R_{wp} = 8.45\%$  (weighted profile factor),  $R_p = 6.733\%$  (profile factor), and  $\chi^2 = 3.5$  (goodness of fit), suggesting a good agreement between measured and refined results. It confirms that the sample is single phase and isostructural to the known Gehlenite-type crystal structure of  $\text{Ca}_2\text{Al}_2\text{SiO}_7$  (JCPDS card No. 35-0755) with tetragonal crystal systems of  $P-421m$  (113) space group. The refined atomic positions and average bond lengths of  $\text{Ca}_2\text{Al}_2\text{SiO}_7$  are listed in **Table 1** and **2**, respectively. The schematic crystal structure is given in the inset of **Fig. 1**. The two-dimensional extended layers are separated by Ca atoms along [011], and three  $[\text{AlO}_4]$  and two  $[(\text{Si}/\text{Al})\text{O}_4]$  tetrahedrons constitute a five-membered ring along [100] with  $\text{Ca}^{2+}$  ions sitting at the center.

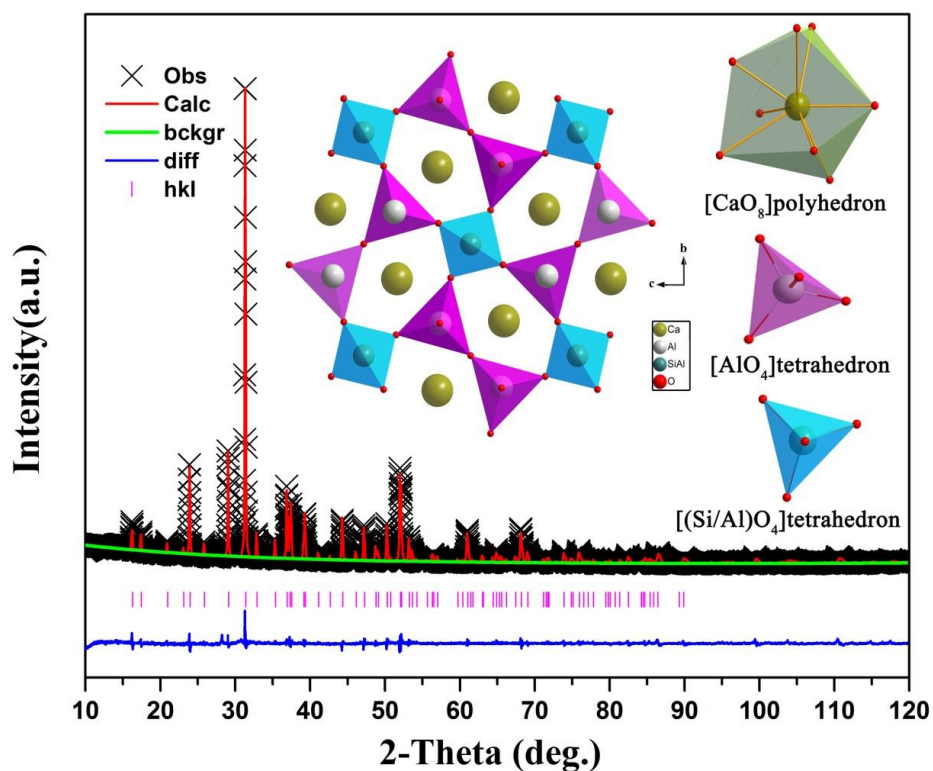


**Fig. 1.** Rietveld refinement of room-temperature XRD data and crystal structure diagram of  $\text{Ca}_2\text{Al}_2\text{SiO}_7$  ceramics sintered at 1440 °C in air.

**Table 1** Atomic positions parameters of  $\text{Ca}_2\text{Al}_2\text{SiO}_7$  by Rietveld refinement.

Atom	Wyckoff	x	y	z	Occupation
Ca1	4e	0.338606	0.161394	0.510039	1
Al1	2a	0	0	0	1
Al2	4e	0.145586	0.354414	0.983638	0.5
Si1	4e	0.142514	0.357486	0.944984	0.5
O1	2c	0.5	0	0.175594	1
O2	4e	0.14296	0.357041	0.275995	1
O3	8f	0.089056	0.168936	0.889741	1

**Table 2** Selected bond length of Ca<sub>2</sub>Al<sub>2</sub>SiO<sub>7</sub> by Rietveld refinement.

Bond	length (Å)	Bond	length (Å)
Ca-O1	2.466(6)	Si O1	1.701(4)
Ca-O2	2.437(5)	Si-O2	1.632(9)
Ca-O3	2.834(4)	Si-O3	1.660(9)
Al2-O1	1.703(9)	Al1-O3	1.7420(9)
Al2-O2	1.632(9)	-	-
Al2-O3	1.659(9)	-	-

The SEM images of Ca<sub>2</sub>Al<sub>2</sub>SiO<sub>7</sub> ceramics sintered at different temperatures are shown in **Fig. 2**. Distribution curve of the grain sizes at different temperatures, calculated by Image J software. The average grain size is found to increase gradually from 1.6μm to 2.4μm with the sintering temperature increase from 1400°C to 1440°C, which is consistent with the evolution of SEM images. **When the sintering temperature further increases to 1460°C, the boundary of grains starts to melt, in that the density start to decrease. Meanwhile, the grains have different grain boundaries and moving speeds, and some of the pores have a lower moving speed than the grain boundaries, which causes the pores to be wrapped in the grains and then abnormal grains appear, at the same time the melting phenomenon of grain edge is observed with the presence of glass phase.**

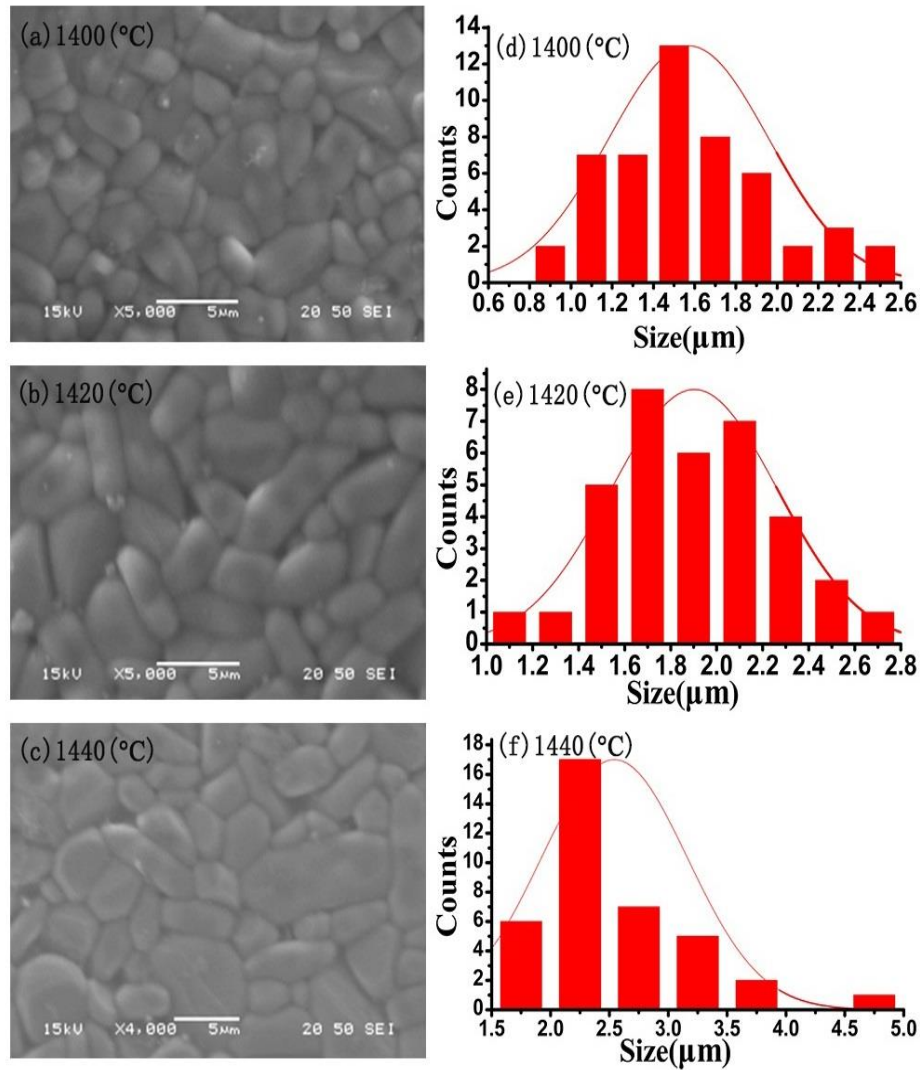


**Fig. 2.A** SEM images of  $\text{Ca}_2\text{Al}_2\text{SiO}_7$  ceramics with different sintering temperatures (a) 1400°C, (b) 1420°C, (c) 1440°C; The distribution of grain size of  $\text{Ca}_2\text{Al}_2\text{SiO}_7$  ceramics at (d) 1400°C, (e) 1420°C, (f) 1440°C.

The relative density ( $\rho_r$ ) and microwave dielectric properties of  $\text{Ca}_2\text{Al}_2\text{SiO}_7$  ceramics as a function of sintering temperature are shown in **Fig. 3**. The values of  $\rho_r$ ,  $Q \times f$  and  $\epsilon_r$  are all increase with the augment of sintering temperature, with maxima of 98%, 22475 GHz and 8.86 achieved at 1440°C, respectively. It is well known that  $Q \times f$  values are dominated by both intrinsic factors (ionic polarization and crystal structure) and extrinsic defects (secondary phases, grain size, and distribution of gain size, grain boundary, oxygen vacancy and porosity) [17]. Here, the high  $Q \times f$  value of 22,457 GHz obtained at 1440°C is mainly



attributed to the increase of both grain size (**Fig. 2.A**) and density (**Fig. 3a**). On the other hand,  $\epsilon_r$  can be corrected according to the Bosman and Havinga's formula [18]:

$$\epsilon_{Bosman} = \epsilon_{Obs} (1+1.5P) , P = 1-\rho_r \quad (2)$$

where,  $P$  is porosity,  $\epsilon_{Bosman}$  and  $\epsilon_{Obs}$  is corrected and observed  $\epsilon_r$ , respectively. The values of  $\epsilon_{Bosman}$  are higher than that of observed as displayed in **Fig. 3(c)**. In addition, the ionic polarizability is dominant to the  $\epsilon_r$  of  $\text{Ca}_2\text{Al}_2\text{SiO}_7$  ceramics, due to the low  $P$  ( $\rho_r > 95\%$ ). **According to the Clausius-Mossotti equation** [19]:

$$\epsilon_{cal} = \frac{3V_m + 8\pi\alpha_D}{3V_m - 4\pi\alpha_D} \quad (3)$$

Where,  $V_m$  is molar volume and  $\alpha_D$  is the ionic polarizability.  $\epsilon_r$  is dominated by each  $\alpha_D$ , which can be calculated from the  $\alpha_D$  of each substance, as follow:

$$\alpha_{th}(\text{Ca}_2\text{Al}_2\text{SiO}_7) = 2\alpha(\text{Ca}^{2+}) + 2\alpha(\text{Al}^{3+}) + \alpha(\text{Si}^{4+}) + 7\alpha(\text{O}^{2-}) \quad (4)$$

$0.472(\text{\AA})^3$ ,  $0.054(\text{\AA})^3$ ,  $0.033(\text{\AA})^3$ , and  $2.75(\text{\AA})^3$  are the ionic polarizabilities of  $\text{Ca}^{2+}$ ,  $\text{Al}^{3+}$ ,  $\text{Si}^{4+}$  and  $\text{O}^{2-}$ , respectively [20]. **The calculated value ( $\epsilon_{cal}$ )  $\sim 7.68$  is lower than the above mentioned  $\epsilon_{Bosman} \sim 9.01$  and  $\epsilon_{Obs} \sim 8.86$ , which should be ascribe to fact that the Clausius-Mossotti equation is more suitable for cubic or isotropic materials other than low symmetry materials** [21]. Furthermore,  $\tau_f$  values are found to slightly decrease from  $\sim -49.16$  ppm/ $^\circ\text{C}$  to  $\sim -51.06$  ppm/ $^\circ\text{C}$  with the increase of sintering temperature (**Fig. 3d**), in relation to the mode of lattice vibration, will be discussed in the later temperature dependent Raman spectra. **The optimum microwave dielectric properties are obtained for  $\text{Ca}_2\text{Al}_2\text{SiO}_7$  ceramic sintered  $1440^\circ\text{C}$  with  $\epsilon_r = 8.86$ ,  $Q \times f = 22,457$  GHz and  $\tau_f = -51.06$  ppm/ $^\circ\text{C}$ .**

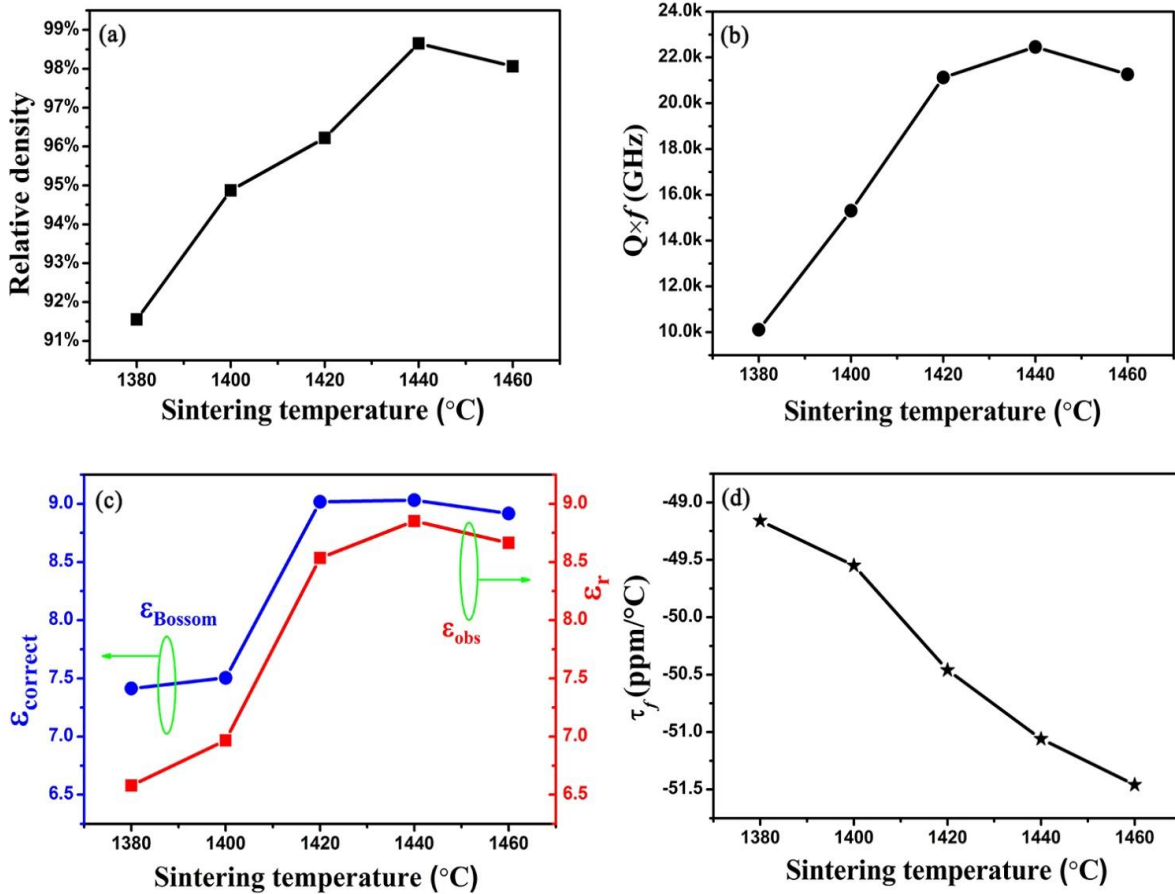


**Fig. 3.** (a) relative density, (b)  $Q \times f$  value, (c) dielectric constants, (d)  $\tau_f$  value of  $\text{Ca}_2\text{Al}_2\text{SiO}_7$  ceramics as a function of sintering temperature.

**Figure 4** exhibits the temperature dependence of  $\epsilon_r$  and dielectric loss ( $\tan\delta$ ) for  $\text{Ca}_2\text{Al}_2\text{SiO}_7$  ceramics at different frequencies from RT to 1000°C. It can be seen that the value of  $\epsilon_r$  and  $\tan\delta$  keeps stable and frequency independence at  $\sim 9$  and  $\sim 10^{-4}$ , respectively, below 310 °C. However, there are two abnormal peaks in  $\epsilon_r$  and  $\tan\delta$  at 100Hz, 1KHz and 10KHz in the temperature range of 400°C-550°C and 700°C-850°C, as shown in **Fig. 4**, which should be related to the low frequency space charge response that clamps out at higher frequencies ( $>1\text{MHz}$ ). There were similar behaviors in  $\text{Ba}_2\text{ZnSi}_2\text{O}_7$  ceramics reported by Zou et al [11]. They gave the  $\epsilon_r$ -T curve from RT to 800 °C, and considered that the abnormal peak band

at 500°C was not a Curie peak, and inferred that  $\text{Ba}_2\text{ZnSi}_2\text{O}_7$  ceramics might have a high  $T_c$  which could be 750°C or higher.

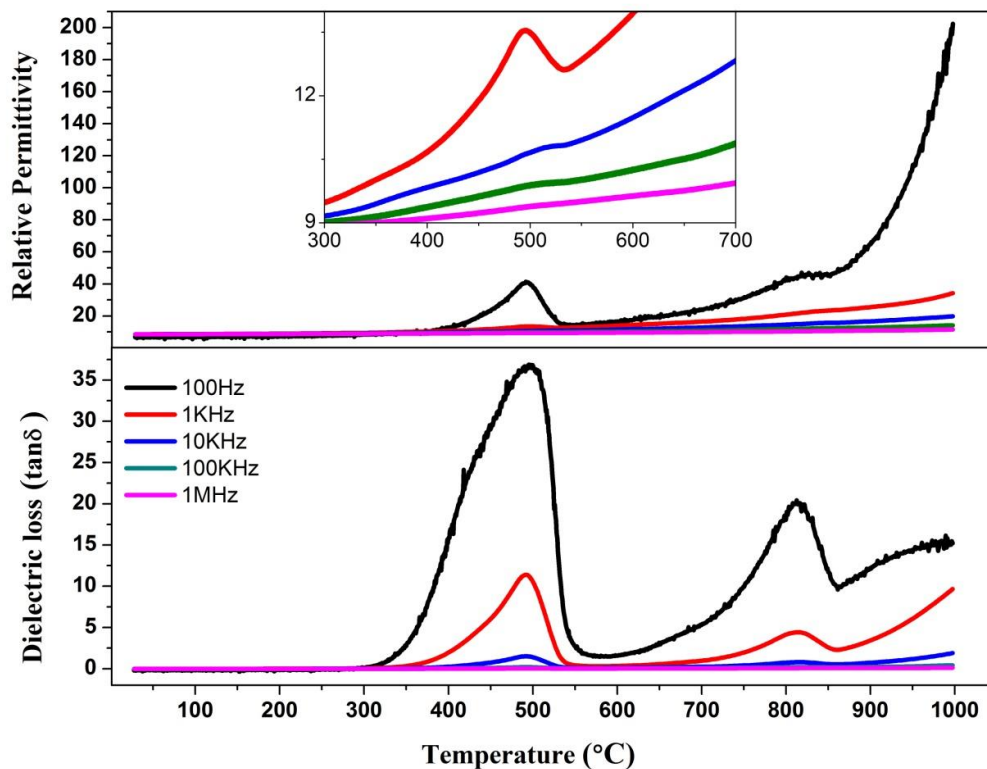


**Fig. 4.** The temperature dependence of dielectric constant and the loss tangent for  $\text{Ca}_2\text{Al}_2\text{SiO}_7$  ceramics.

The XRD patterns of  $\text{Ca}_2\text{Al}_2\text{SiO}_7$  as a function of different testing temperatures have been given in **Fig. 5**, all diffraction peaks of which are matched well with the standard JCPDS card No. 35-0755. No phase transition or any secondary phase is observed with the temperature increasing from room temperature to 900°C.

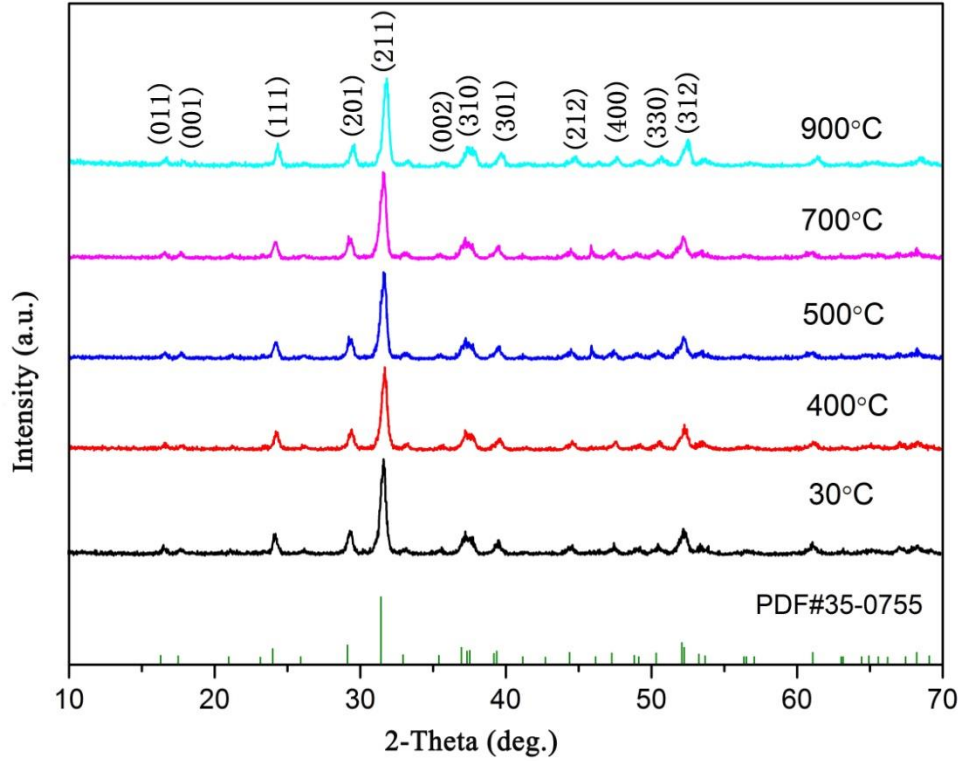


**Fig. 5.** The XRD patterns of  $\text{Ca}_2\text{Al}_2\text{SiO}_7$  ceramics as a function of testing temperature.

Further, *in-situ* temperature dependence of Raman spectra of  $\text{Ca}_2\text{Al}_2\text{SiO}_7$  ceramics from 100°C to 600°C is shown in **Fig. 5**. There are no obvious clues of phase transition in *in-situ* Raman profiles except slight blue shift at the range of 200nm-300nm wavenumbers, in agreement with the *in-situ* XRD results (**Fig. 5**). According to the group theory and irreducible representations, there are 45 different Raman vibrational modes (optical branches) in  $\text{Ca}_2\text{Al}_2\text{SiO}_7$  [22]:

$$\Gamma_{\text{optic}} = 10A_{1g} + 7B_{1g} + 10B_{2g} + 18E \quad (5)$$

The symmetry species of vibrational modes contributed by each set of four equivalent atoms which occupy sites of symmetry  $C_s$  are  $2A_{1g} + 2B_{1g} + 2B_{2g} + 3E$ , there are three such sets: Ca, (Al2/Si) and O2. The O1 of site symmetry  $C_1$  contributions are  $3A_{1g} + 3B_{2g} + 6E$ . The Al1 atoms of the site symmetry  $S_4$  contributions are  $B_{1g} + B_{2g} + 2E$ . The O3 of site symmetry  $C_{2v}$  contributions are  $A_{1g} + B_{2g} + 2E$ . In the above vibration mode,

220 $\text{cm}^{-1}$  and 320  $\text{cm}^{-1}$  bands can be assigned to the stretching vibrations of Ca-O bond, corresponding to the O-Ca-O bending in  $\text{CaO}_8$  polyhedron [23]. The strongest band at 624 $\text{cm}^{-1}$  is a symmetrical stretching [ $\nu_s(\text{Al-O-Al})$ ] mode of bridging oxygen of the pyrosilicate anions. The band at 800  $\text{cm}^{-1}$  is antisymmetric stretch [ $\nu_{as}(\text{Al-O-Al})$ ] modes involving  $\text{AlO}_4$  tetrahedra. The 910 $\text{cm}^{-1}$  and 974 $\text{cm}^{-1}$  bands are attributed to symmetric stretch mode of [ $\nu_s(\text{T-O-T})$ ](where T:Si or Al) nonbridging oxygen and antisymmetric stretch mode of oxygen of the pyrosilicate group [ $\nu_{as}(\text{Si-O-Si})$ ]. Especially, with the increase of temperature from room temperature to 600 $^{\circ}\text{C}$ , the Raman bands at 220  $\text{cm}^{-1}$  and 320  $\text{cm}^{-1}$  shift slightly towards low wave numbers. It hints that it is the main affecting factor of  $Q \times f$  and  $\tau_f$  change as a function of temperature for the stretching vibrations of Ca-O bond and O-Ca-O bending in  $\text{CaO}_8$  polyhedron.

Therefore, as shown in **Fig. 5** and **6**, the tests of variable temperature XRD and Raman demonstrate there are no phase change for  $\text{Ca}_2\text{Al}_2\text{SiO}_7$  from RT to 900 $^{\circ}\text{C}$  and 600 $^{\circ}\text{C}$ , considering  $\text{Ca}_2\text{Al}_2\text{SiO}_7$  has the same structure with  $\text{Ba}_2\text{ZnSi}_2\text{O}_7$ . There are the two abnormal peak bands centered at 500  $^{\circ}\text{C}$  and 800  $^{\circ}\text{C}$ , which are attributed to space charge polarization. we think that the first abnormal peak at 500  $^{\circ}\text{C}$  is the Debye Relaxation peak, the highest point is the Debye Relaxation extreme point, which is inversely proportional to the frequency, and its peak shifts with temperature to the high temperature region, that is in line with the trend of dielectric loss in the fig4. The second peak at 800 $^{\circ}\text{C}$  is the sample with a higher frequency is affected by weak fluctuations [11]. So the  $T_c$  of  $\text{Ca}_2\text{Al}_2\text{SiO}_7$  ceramics is above 900 $^{\circ}\text{C}$ .

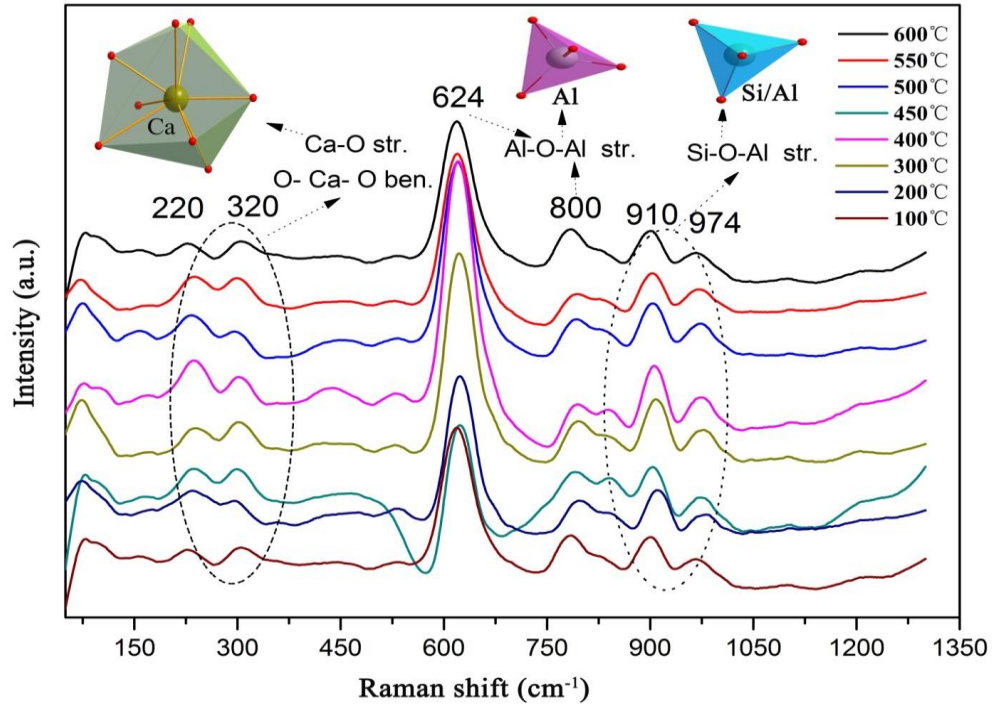


**Fig. 6.** Raman spectra for  $\text{Ca}_2\text{Al}_2\text{SiO}_7$  ceramics as a function of temperature.

## 4 Conclusion

Gehlenite typed  $\text{Ca}_2\text{Al}_2\text{SiO}_7$  ceramics were successfully fabricated by the conventional solid-state reaction method. Rietveld refinement of XRD patterns indicated that  $\text{Ca}_2\text{Al}_2\text{SiO}_7$  was a tetragonal crystal structure with a space group of  $P-421m$  (113). There are 6 main activity modes in Raman spectra, which have been attributed to the vibration of Ca-O and O-Ca-O and  $\nu_s$  (Al-O-Al) and  $\nu_{as}$  (Si-O-Si). The *in-situ* temperature dependence of XRD patterns, Raman spectra and dielectric properties demonstrated that no phase transition was found to happen in  $\text{Ca}_2\text{Al}_2\text{SiO}_7$  ceramics from RT to 900 °C. Two dielectric abnormal peaks were observed in low frequencies at the temperature range of 400°C-550°C and 700 °C-850°C,  $T_c$  of  $\text{Ca}_2\text{Al}_2\text{SiO}_7$  ceramics is above 900°C. The optimum microwave properties of  $\text{Ca}_2\text{Al}_2\text{SiO}_7$  ceramics ( $\epsilon_r = 8.86$ ,  $Q \times f = 22,457\text{GHz}$ , and  $\tau_f = -51.06 \text{ ppm/}^\circ\text{C}$ ) were achieved on the samples sintered at 1440°C,

indicating its possible usage in millimeter wave communication systems including capacitors and microwave substrates.

## Acknowledgements

This work was supported by the National Natural Science Foundation of China under grant number: 51672063, 51202051. Open projects of Key Laboratory of inorganic functional materials and devices, Shanghai silicate institutes, Chinese academy of sciences under grant number: KLIFMD201708.

## References

- [1] L.J. Chen, L. Liu, Q. Ma, S.J. Liu, Relationship between densification behavior and stabilization of quasi-liquid grain boundary layers in CuO-doped  $0.7\text{CaTiO}_3\text{-}0.3\text{NdAlO}_3$  microwave ceramics, *Acta.Mater.*111 (2016) 102.
- [2] J.B. Song, K.X. Song, J.S. Wei, H.X. Lin, J. Wu, Ionic occupation, structures, and microwave dielectric properties of  $\text{Y}_3\text{MgAl}_3\text{SiO}_{12}$  garnet-type ceramics, *J. Am. Ceram.Soc.*101 (2018) 244.
- [3] H. Sun, Y.X. Lu, X. Xie, T.S. Yao, Z. Xu, Y. Wang, Structural, magnetic, and dielectric properties in Aurivillius phase  $\text{Sr}_x\text{Bi}_{6-x}\text{Fe}_{1-x/2}\text{Co}_{1-x/2}\text{Ti}_{3+x}\text{O}_{18}$ , *J. Eur. Ceram.Soc.*39 (2019) 2103.
- [4] Y. Tang, M.Y. Xu, L. Duan, J.Q. Chen, Structure, microwave dielectric properties, and infrared reflectivity spectrum of olivine type  $\text{Ca}_2\text{GeO}_4$  ceramic, *J Soc. Eur. Ceram.*39 (2019) 2354.
- [5] X.K. Lan, J. Li, Z.Y. Zhou, W.Z. Lu, W. Lei, Lattice structure analysis and optimised microwave dielectric properties of  $\text{LiAl}_{1-x}(\text{Zn}_{0.5}\text{Si}_{0.5})_x\text{O}_2$  solid solutions, *J. Eur. Ceram.Soc.*39 (2019) 2360.

- [6] Y.H. Zhang, J.J. Sun, N. Dai, Z.C. Wu, Z.H. Wu, Crystal structure, infrared spectra and microwave dielectric properties of novel extra low-temperature fired  $\text{Eu}_2\text{Zr}_3(\text{MoO}_4)_9$  ceramics, *J. Eur. Ceram.Soc.*39 (2019) 1127.
- [7] W.C. Tsai, K.C. Chiu, Y.X. Nian, Y.C. Liou, Significant improvement of the microwave dielectric loss of  $\text{Zn}_{1.95}\text{M}_{0.05}\text{SiO}_4$  ceramics (M=Zn, Mg, Ni, and Co) prepared by reaction-sintering process, *J. Mater.Sci.Mater.Electron.*28 (2017) 14258.
- [8] C. Zhang, R.Z. Zuo, J. Zhang, Y. Wang, Structure-Dependent Microwave Dielectric Properties and Middle-Temperature Sintering of Forsterite ( $\text{Mg}_{1-x}\text{Ni}_x$ ) $_2\text{SiO}_4$  Ceramics, *J. Am. Ceram.Soc.*98 (2015) 702.
- [9] X.H. Ma, S.H. Kweon, S. Nahm, Low-temperature sintering and microwave dielectric properties of  $\text{B}_2\text{O}_3$ -added ZnO-deficient  $\text{Zn}_2\text{GeO}_4$  ceramics for advanced substrate application, *J. Eur. Ceram.Soc.*38 (2015) 4682.
- [10] K.X. Song, S. Wu, P. Liu, et al. Phase composition and microwave dielectric properties of  $\text{SrTiO}_3$ , modified  $\text{Mg}_2\text{Al}_4\text{Si}_5\text{O}_{18}$ , cordierite ceramics. *J Alloys Compd.* 628 (2015) 57.
- [11] Z.Y. Zou, X.K. Lan, W.Z. Lu, G.F. Fan, X.H. Wang, X.C. Wang, P. Fu, W. Lei, Novel high Curie temperature  $\text{Ba}_2\text{ZnSi}_2\text{O}_7$  ferroelectrics with low-permittivity microwave dielectric properties, *Ceram.Int.*42 (2016) 16387.
- [12] P. Florian, E. Veron, T.F.G. Green, J.R. Yates, D. Massiot, Elucidation of the Al/Si Ordering in Gehlenite  $\text{Ca}_2\text{Al}_2\text{SiO}_7$  by Combined Si-29 and Al-27 NMR Spectroscopy/Quantum Chemical Calculations, *Chem. Mater.*24 (2012) 4068.



- [13] H. Takeda, M. Hagiwara, H. Noguchi, T. Hoshina, T. Takahashi, N. Kodama, Calcium aluminate silicate  $\text{Ca}_2\text{Al}_2\text{SiO}_7$  single crystal applicable to piezoelectric sensors at high temperature, *Appl. Phys. Lett.* 102 (2013) 3153.
- [14] A.M. Lejus, N. Pelletier-Allard, R. Pelletier, D. Vivien, Site selective spectroscopy of Nd ions in gehlenite ( $\text{Ca}_2\text{Al}_2\text{SiO}_7$ ), a new laser material, *Opt. Mater.* 6 (1996) 29.
- [15] B.H. Toby, EXPGUI, A graphical user interface for GSAS, *J. Appl. Cryst.* 34 (2001) 210.
- [16] H.M.J. Rietveld, A profile refinement method for nuclear and magnetic structures, *J. Appl. Cryst.* 2 (1969) 65.
- [17] S.D. Ramarao, S.R. Kiran, V.R.K. Murthy, Structural, lattice vibrational, optical and microwave dielectric studies on  $\text{Ca}_{1-x}\text{Sr}_x\text{MoO}_4$ , ceramics with sheltie structure, *Mater. Res. Bull.* 56 (2014) 71.
- [18] S.H. Yoon, D.W. Kim, S.Y. Cho, K.S. Hong, Investigation of the relations between structure and microwave dielectric properties of divalent metal tungstate compounds, *J. Eur. Ceram. Soc.* 26 (2006) 2051.
- [19] R.D. Shannon, Dielectric polarizabilities of ions in oxides and fluorides, *J. Appl. Phys.* 73 (1993) 348.
- [20] L. Pauling, The theoretical prediction of the Physical Properties of Many-Electron Atoms and Ions. Mole Refraction, Diamagnetic Susceptibility, and Extension in Space, *Proc Roy. Soc(A)*, 114 (1927) 191.
- [21] X.Q. Song, W.Z. Lu, X.C. Wang, X.H. Wang, G.F. Fan, R. Muhammad, W. Lei, Muhammad, W. Lei, Sintering behaviour and microwave dielectric properties of  $\text{BaAl}_{2-2x}(\text{ZnSi})_x\text{Si}_2\text{O}_8$  ceramics, *J. Eur. Ceram. Soc.* 38(2018) 1529.
- [22] Z. Burshtein, Y. Shimony, S. Morgan, D.O. Henderson, R. Mu, E. Silberman, Symmetry lowering due to site-occupation disorder in vibrational spectra of gehlenite,  $\text{Ca}_2(\text{AlSi})\text{AlO}_7$ , *Phys. Chem. Solids.* 54 (1993) 1043.

[23] S.K. Sharma, B. Simons, H.S. Yoder, Raman study of anorthite, calcium Tschermak's pyroxene, and gehlenite in crystalline and glassy states, *Am.Mineral.*68 (1983) 1113.